DOI: 10.1002/ejic.201001351

Carborane-Derivatized Low-Melting Salts with Ether-Functionalized Cations – Preparation and Properties

Shimin Liu,[a,b] Zhengjian Chen,[a] Qinghua Zhang,[a] Shiguo Zhang,[a] Zuopeng Li,[a] Feng Shi,[a] Xiangyuan Ma,[a] and Youquan Deng*[a]

Keywords: Ionic liquids / Carboranes / Boron / Carbon / Raman spectroscopy / IR spectrocsopy

A new series of low-melting ammonium salts based on the [*nido*-7,8-$C_2B_9H_{12}$]$^-$ anion have been synthesized and characterized, and their physicochemical properties including spectroscopic properties, thermal properties, surface properties, solubility, density, viscosity, electrochemical properties, and tribological properties have been studied in detail. In comparison with previously reported carborane-derivatized imidazolium or pyridinium salts, these diether-functionalized ammonium salts display lower phase transition temperatures (T_g = –76 to –57 °C), and four exist as liquids at room temperature due to their flexible alkoxy chains. TGA analysis revealed that the weight loss rates of these carborane-derivatized low-melting salts were ca. 30–80 wt.-% after thermal decomposition, which is different from the traditional RTILs. SEM images showed that the resulting residue had hollow reticular shell morphology, and XPS and XRD analyses indicate that the main components of the skeleton are B_2O_3 and amorphous carbon. This provides a new strategy for preparing new inorganic porous materials by thermal decomposition of these low-melting salts.

Introduction

In the past decade, low-melting salts (i.e. ionic liquids, ILs) have received a great deal of attention as they exhibit some unique properties including low volatility, good thermal and electrochemical stability, excellent ion conductivity, and tunable characteristics.[1] This interest is driving a rapid increase in developing novel ILs, and up to now, thousands of ILs with unique physicochemical features and functions have been developed. The continued enthusiasm for ILs stems largely from their potential applications in the chemical industry, e.g. as catalysts or reaction media in large-scale catalytic processes,[2] as electrolytes in electrochemical devices or processes,[3] as high performance additives in paints,[4] plastics,[5] and cleaning agents,[6] as modifiers in medicine (coated implants), food analytics, and sensors.[7] Currently, it has been recognized that the applications of ILs are not only confined to the chemical engineering fields, and the special performance of ILs as soft functional materials in many areas including light-emitting materials,[8] magnetic fluids,[9] lubricants,[10] heat storage/heat transfer fluids[11] is receiving more interest in both academia and industry.

Carboranes, a peculiar class of inorganic compounds with the structure of carbon-containing polyhedral boron-cluster, have attracted massive interest due to their unique three-dimensional rigid cluster structure and their resulting properties.[12] They are widely applied in a variety of areas, especially catalysis and coordination chemistry.[13] Importantly, ionic carborane derivatives have potential utility as tumour targeting reagents in boron–neutron capture therapy or liquid neutron moderators in nuclear processing. As some anionic boron clusters have delocalized charge characteristics, extraordinarily weak nucleophilicity, and relative chemical inertness,[14] they have been explored in combination with bulky cations (e.g. imidazolium and pyridinium) to form organic salts with melting points below 150 °C. For example, some imidazolium and pyridinium salts with anionic boron clusters including [*closo*-$CB_{11}H_{12}$]$^-$,[15–17] [*nido*-7,8-$C_2B_9H_{12}$],[17,18] [*closo*-1,2-$C_2B_{10}H_{11}$]$^-$,[19] and [$Co(C_2B_9H_{11})_2$]$^-$,[18] have been reported. In comparison with common anions such as [BF_4]$^-$, [PF_6]$^-$, [$N(CN)_2$]$^-$, and [NTf_2]$^-$, some anionic boron clusters possess weaker coordinating ability and higher chemical inertness. However, their corresponding imidazolium and pyridinium salts exhibit the relatively high melting points due to the inherently rigid anions. To the best of our knowledge, most of the reported salts with a carborane anion are solids at room temperature except some imidazolium salts with the [$Co(C_2B_9H_{11})_2$]$^-$ anion, which are viscous liquids (ca. 10^4 cP at 25 °C).[18] Thus it would limit their application in many fields as liquid functional materials. Additionally, as an important member of IL family, studies on the properties of these novel ILs with a carborane moiety are far less extensive than common

[a] Centre for Green Chemistry and Catalysis, Lanzhou Institute of Chemical Physics, Chinese Academy of Sciences, Lanzhou 730000, China
Fax: +86-931-4968116
E-mail: ydeng@licp.cas.cn
[b] Graduate School of the Chinese Academy of Sciences, Beijing 100039, China

Supporting information for this article is available on the WWW under http://dx.doi.org/10.1002/ejic.201001351.

ILs. Therefore, the development of new low-melting salts with a carborane anion, and in-depth studies of their physicochemical properties are very desirable.

In previous reports, the imidazolium and pyridinium salts based on the [*nido*-7,8-$C_2B_9H_{12}$]$^-$ anion exhibited comparatively lower melting points than those based on [*closo*-$CB_{11}H_{12}$]$^-$,[17] the melting points of the former ranged mainly from 40 °C to 150 °C, and no liquid examples have been reported. Recently, Matsumoto et al. reported ether-functionalized ILs and found that the introduction of an alkoxy group into the quaternary ammonium could reduce the melting point and viscosity of the ILs.[20] Inspired by this progress, we have combined five diether-substituted ammonium cations with the dodecahydrodicarba-*nido*-undecaborate "dicarbollide" anion, [*nido*-7,8-$C_2B_9H_{12}$]$^-$, to obtain room temperature ionic liquids (RTILs). Moreover, their spectroscopic characteristics, thermal properties, surface properties, solubility, density, viscosity, electrochemical properties, and tribological properties have been studied. The structures and abbreviations of the cations and the [*nido*-7,8-$C_2B_9H_{12}$]$^-$ anion are shown in Scheme 1.

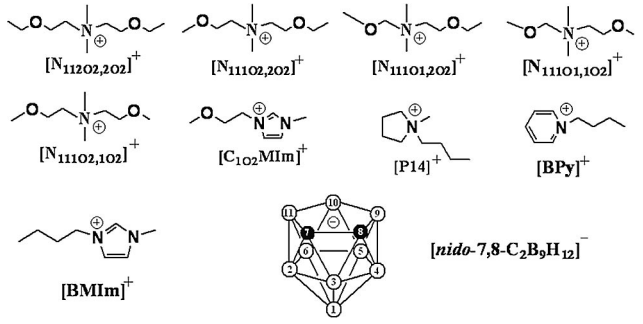

Scheme 1. The structures and abbreviations of the cations and anion in this work.

Results and Discussion

Preparation

All the ILs based on [*nido*-7,8-$C_2B_9H_{12}$]$^-$ were synthesized by metathesis reactions from halide (Cl^- or Br^-) precursors and equimolar amounts of the cesium carborane salt, Cs[*nido*-7,8-$C_2B_9H_{12}$], which was synthesized through deboronation of *o*-carborane with strong base.[21] In this study, [$N_{111O1,2O2}$][*nido*-7,8-$C_2B_9H_{12}$] and [$N_{111O1,1O2}$][*nido*-7,8-$C_2B_9H_{12}$] were obtained from the chloride precursors and the remaining ILs were prepared from bromide precursors. All the carborane-derivatized ILs were synthesized with yields of 82–90% (based on *o*-carborane), and they are air and moisture stable. Among them, [$N_{112O2,2O2}$][*nido*-7,8-$C_2B_9H_{12}$], [$N_{111O2,2O2}$][*nido*-7,8-$C_2B_9H_{12}$], [$N_{111O1,2O2}$][*nido*-7,8-$C_2B_9H_{12}$], and [$N_{111O1,1O2}$][*nido*-7,8-$C_2B_9H_{12}$] are colourless or pale yellow liquids, and [$N_{111O2,1O2}$][*nido*-7,8-$C_2B_9H_{12}$], [C_{1O2}MIm][*nido*-7,8-$C_2B_9H_{12}$], and [P14][*nido*-7,8-$C_2B_9H_{12}$] are white waxy solids at room temperature. The bromide content of the ionic liquids synthesized from bromide precursors was less than 0.2% w/w. The chloride content of the two ionic liquids synthesized from chloride precursors was not measured because of the ion interference of [*nido*-7,8-$C_2B_9H_{12}$]$^-$. In order to ensure that the salts were free from water, the ILs were kept in a vacuum (pressure 10^{-2}–10^{-3} mbar) at 90–100 °C for 10 h for the removal of water before every test. As the [*nido*-7,8-$C_2B_9H_{12}$]$^-$ anion reacts with iodine in methanol solution slowly, the water content of all carborane-derivatized ILs was less than 1000 ppm, directly determined by the Karl Fischer method.

NMR Measurements

Firstly, the NMR spectroscopy was used to characterize the structures of the ILs prepared, and the information obtained showed that all the compounds were as expected. As the ^{1}H NMR spectra of [$N_{112O2,2O2}$][*nido*-7,8-$C_2B_9H_{12}$] in Figure 1 (a) shows, the chemical shifts of the hydrogen atoms in the [$N_{112O2,2O2}$]$^+$ cation are mainly located in the narrow field of 3.3–4.1 ppm with the exception of a multiple peak attributed to two CH_3 groups in the alkoxy chains, which was observed at approximately 1.2 ppm. Moreover, the [*nido*-7,8-$C_2B_9H_{12}$]$^-$ anion gave two representative resonances in the deuterated acetone: (1) the chemical shifts of $C_{cluster}$–H was located at approximately 1.7 ppm, and (2) the signal of the B–H–B bridging hydrogen atoms was a broad peak ranging from –3.2 to –2.6 ppm, which was weak and could not be found easily.[22] The ^{13}C NMR spectra (Figure 1, b) showed five strong peaks, which can be assigned to the five types of carbon atom in the [$N_{112O2,2O2}$]$^+$ cation. These peaks, ascribed to the anion, were located at approximately 42–43 ppm.[23] The ^{11}B {^{1}H} NMR spectrum for the [*nido*-7,8-$C_2B_9H_{12}$]$^-$ anion is shown in Figure 1 (c), from which six peaks can be observed at δ = –10.9, –16.3, –17.1, –21.8, –32.9, and –37.7 ppm, which were assigned to B (9,11), B (5,6), B (3), B (2,4), B(10), and B (1), respectively. The ^{11}B {^{1}H} NMR spectrum for the [*nido*-7,8-$C_2B_9H_{12}$]$^-$ anion is consistent with the expected structure.[24]

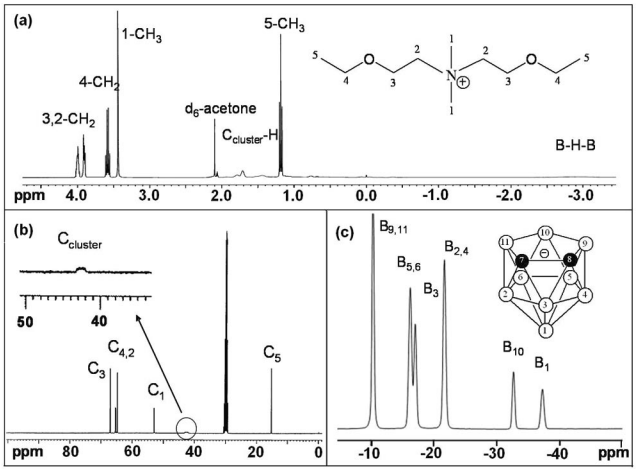

Figure 1. ^{1}H, (a) ^{13}C (b) NMR spectra of [$N_{112O2,2O2}$][*nido*-7,8-$C_2B_9H_{12}$] and ^{11}B {^{1}H} (c) NMR spectrum of the anionic boron cluster.

Vibrational Spectra

In order to investigate the spectral pattern of the new ILs based on the *nido*-structure, we measured their IR and Raman spectra. Figure 2 shows typical FTIR and Raman spectra for $[N_{112O2,2O2}][nido\text{-}7,8\text{-}C_2B_9H_{12}]$, which is a good example of the infrared absorption of the new ILs, and the assignment of the various groups of spectra features are marked.

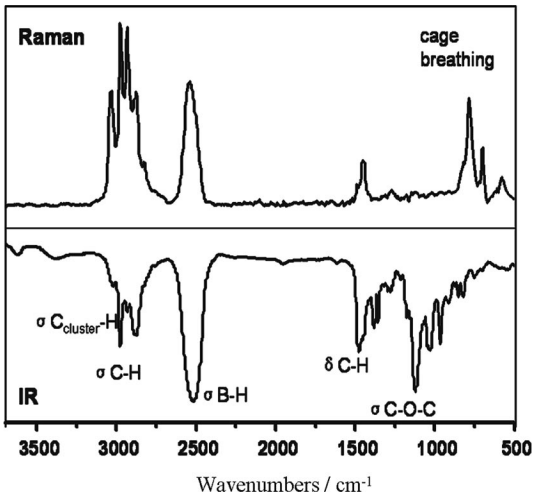

Figure 2. FTIR and Raman spectra of the $[N_{112O2,2O2}][nido\text{-}7,8\text{-}C_2B_9H_{12}]$.

Two characteristic absorptions for the $[nido\text{-}7,8\text{-}C_2B_9H_{12}]^-$ anion were detected in both IR and Raman spectra: an absorption in the range of 3020–3030 cm^{-1} can be attributed to the C–H stretching vibrations of the anion, and a very strong peak in the range of 2500–2520 cm^{-1} is ascribed to the B–H stretches.[25] Compared to the stretching frequencies of B–H situated in closo *o*-carborane cages, the σ bond in the open face of the *nido* polyhedron generally induces a redshift, which is consistent with that seen previously.[25] For the diether-substituted ammonium cations, the absorption of the asymmetric C–H stretch of the methyl and methylene groups were observed from 2850–3000 cm^{-1}, and the peak due to deformation vibrations of the methylene groups occurs at 1470 cm^{-1}. These vibrations are both IR and Raman active. As for the C–O–C stretching vibrations, an obvious absorption appears at 1120 cm^{-1}. The fingerprints of icosahedral carboranes, namely, the most intense Raman line corresponding to the cage breathing vibration, were observed in the Raman spectrum in the region of 750–800 cm^{-1} and have no IR analogue. Thus, in order to obtain a detailed spectral pattern of the carborane derivatives, combining FTIR and Raman spectra is highly effective.

Surface Properties

Surface properties of the materials are very important for understanding many mechanisms, in particular those involving interface chemistry of the materials. Therefore, X-ray photoelectron spectroscopy (XPS) is a powerful tool for acquiring surface information of the ILs and was used to examine the surface compositions and the element valences.[26] As expected, under the analysis conditions, all the carborane-derivatized ILs showed well defined characteristic emissions, and no visible degradation was observed during or after measuring, indicating that these samples are stable during exposure to the X-ray and ultra-high vacuum conditions.

Figure 3 gives an overview of the scan of a $[N_{111O2,2O2}][nido\text{-}7,8\text{-}C_2B_9H_{12}]$ film and the high resolution B 1s and C 1s spectra. The XPS survey spectrum showed the presence of boron, carbon, nitrogen, and oxygen. Besides that, traces of Si-containing contaminants were detected, which might originate from the sealing of the storage container or silicone grease introduced during synthesis.[27] As shown in Figure 3 (b), the B 1s spectrum displays one peak at binding energy of 188.8 eV. The binding energy of B 1s in $[N_{111O2,2O2}][nido\text{-}7,8\text{-}C_2B_9H_{12}]$ is higher than that in $Cs[nido\text{-}7,8\text{-}C_2B_9H_{12}]$ (188.3 eV), indicating that the charge density of the anion in the IL is lower than that in the cesium salt due to the influence of a different cation.[28] Curve-fitted XPS spectra of C 1s are shown in Figure 3 (c), which exhibit at least three different types of carbon atom in the structure of the IL. The first component can be attributed to carbon atoms in C–C and C–H bonds at 284.6 eV; the second can be assigned to carbon atoms in C–N bonds at 285.6 eV; and the third component is consistent with the carbon atoms in C–O bonds in the cation and C–B bonds in the anion (the C 1s electrons have the same binding energy at 286.5 eV in both C–O and C–B bonds).[29] As for the O 1s and N 1s spectrum, only one peak was observed, and the binding energies of the core electrons were 532.6 and 403.0 eV, respectively. The XPS survey spectra of other prepared functional ILs is similar to $[N_{111O2,2O2}][nido\text{-}7,8\text{-}C_2B_9H_{12}]$, and the binding energies of the elements only changed slightly. Taking $[C_{1O2}MIm]$-

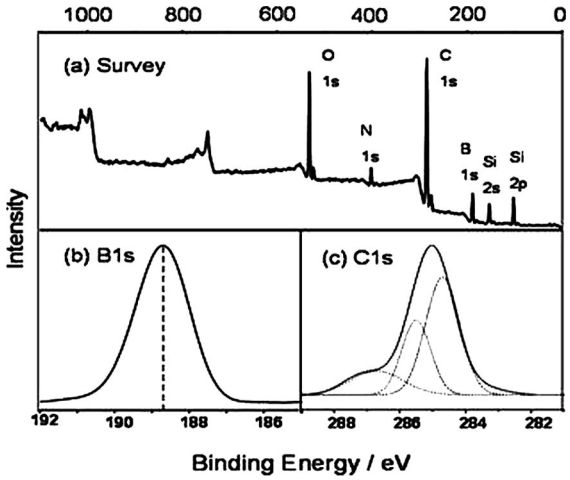

Figure 3. XPS spectra for the survey and B1s, C1s regions of $[N_{111O2,2O2}][nido\text{-}7,8\text{-}C_2B_9H_{12}]$.

[*nido*-7,8-$C_2B_9H_{12}$] as the example, the binding energies of B 1s, O 1s, and N 1s are 188.7, 532.5, and 402.3 eV, respectively.

Thermal Properties

The thermal properties of the carborane-derivatized ILs including melting point (T_m), glass transition (T_g), enthalpy change, heat capacity (C_p), and thermal stability were investigated by differential scanning calorimetry (DSC) and thermogravimetric analysis (TGA), and the data are listed in Table 1.

For the four RTILs based on the [*nido*-7,8-$C_2B_9H_{12}$]$^-$ anion (Table 1, entries 1–4), i.e. [$N_{112O2,2O2}$][*nido*-7,8-$C_2B_9H_{12}$], [$N_{111O2,2O2}$][*nido*-7,8-$C_2B_9H_{12}$], [$N_{111O1,2O2}$][*nido*-7,8-$C_2B_9H_{12}$], and [$N_{111O1,1O2}$][*nido*-7,8-$C_2B_9H_{12}$], a significant feature arising from their phase behavior is that they only exhibited glass-forming characteristics without the observation of melting or crystallization (Figure 4, a). Differing from the first behavior, except for a glass transition in a cooling and heating cycle, cold crystallization occurred during the heating process for [$N_{111O2,1O2}$][*nido*-7,8-$C_2B_9H_{12}$] (5 °C) and [C_{1O2}MIm][*nido*-7,8-$C_2B_9H_{12}$] (–11 °C), which melted at 49 and 43 °C, respectively (Figure 4, b). The DSC traces showed that the phase behavior of [BMIm][*nido*-7,8-$C_2B_9H_{12}$] also shows these features. In addition, both [BPy][*nido*-7,8-$C_2B_9H_{12}$] (Figure 4, c) and [P14][*nido*-7,8-$C_2B_9H_{12}$] (Figure 4, d) displayed a melting and a crystallization in the cooling and heating cycle. The T_m of [BPy][*nido*-7,8-$C_2B_9H_{12}$] (55 °C) tested in this work is slightly higher than the reported value (49 °C).[17] However, two solid crystallines phases were observed from the DSC trace. This phenomenon indicates that a mutual conversion between the two different crystalline structures occurred in the IL as the temperature was changed, which might be caused by dynamically disordered orientations of IL constituents about the molecular axis.[30]

As already noted, most of the imidazolium and pyridinium ILs based on carborane anions are solids at room temperature. It has been recognized that the melting point of an IL is determined mainly by molecular symmetry, intermolecular forces, and conformational degrees of freedom of the molecule.[31] It was expected that introduction of the alkoxy group would reduce the melting point of the ILs, however, in comparison with [BMIm][*nido*-7,8-$C_2B_9H_{12}$] (T_m = 39 °C), [C_{1O2}MIm][*nido*-7,8-$C_2B_9H_{12}$] exhibited a higher melting point (T_m = 43 °C), although the cold-crystal temperature of the latter (T_c = –11 °C) was lower than that of the former (T_c = 11 °C). Analyzing the reason, we suspect that, although the introduction of the more flexible isoelectronic ether group increased the conformational degrees of freedom of the molecule to a certain extent, the enhancement in hydrogen bonding interactions caused by the alkoxy group dominates, thereby resulting in the increase of the T_m. At the same time, after introducing two alkoxy groups into the ammonium cations, four viscous liquids were obtained at room temperature, though their melting points were not observed. This might be explained by the higher flexibility, lower symmetry, and relatively larger size of the cations due to the introduction of two alkoxy groups, which decrease the packing efficiency and predominate over the influence caused by corresponding increase of van der Waals interactions.[32] Moreover, [$N_{111O2,1O2}$][*nido*-7,8-$C_2B_9H_{12}$] is a waxy solid at room temperature (T_m = 41 °C), which is mainly due to its relatively high cation symmetry compared to other four diether-functionalized ILs.

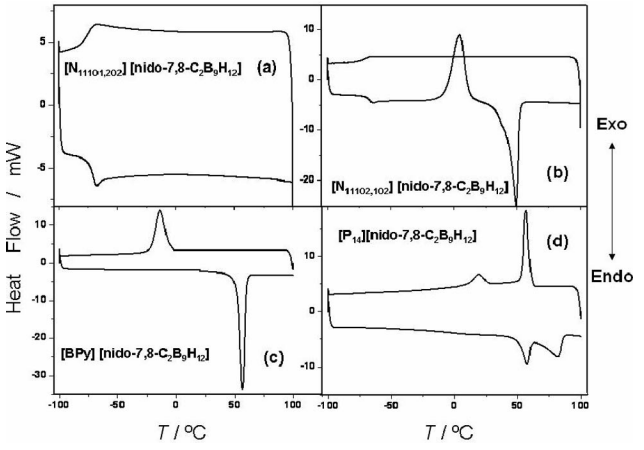

Figure 4. Representative DSC curves of the carborane-derivatized ILs.

Table 1. The thermal properties of [*nido*-7,8-$C_2B_9H_{12}$]$^-$.

Cations	T_g [a] [°C]	T_f [b] [°C]	ΔH_f [c] [J/g]	T_m [d] [°C]	ΔH_m [e] [J/g]	C_p [f] [J/g/K]	T_d [g] [°C]
[$N_{112O2,2O2}$]$^+$	–64					2.04	227
[$N_{111O2,2O2}$]$^+$	–63					2.07	211
[$N_{111O1,2O2}$]$^+$	–71					2.12	175
[$N_{111O1,1O2}$]$^+$	–76					1.99	202
[$N_{111O2,1O2}$]$^+$	–67	5 [h]	83	49	–83	2.07	232
[C_{1O2}MIm]$^+$	–57	–11 [h]	64	43	–67	– [j]	343
[P14]$^+$		19	10	81	–18	2.14	265
[BPy]$^+$		–13	64	55 [i]	–97	– [j]	293
[BMIm]$^+$	–64	11 [h]	50	39	–51	– [j]	274

[a] Glass transition temperature. [b] Freezing point. [c] Freezing enthalpy. [d] Melting point. [e] Melting enthalpy. [f] Heat capacity at 25 °C. [g] Thermal decomposition temperature. [h] Cold-crystal temperature. [i] Reported value is 49 °C in ref.[17] [j] not detected due to phase transition at about 25 °C.

According to previous reports, ILs are good glass formers, which can be cooled from the equilibrium liquid state down to low temperatures without crystallizing, entering the metastable supercooled liquid state, undergoing a glass transition leading to an out-of-equilibrium glassy state.[33] Among the ILs studied in this work, all the ether-functionalized ILs exhibited glass-forming behavior during the cooling and heating cycle, and their T_g ranged from –76 to –57 °C. The four diether-substituted ammonium ILs do not show any other feature except a glass transition due to large dimensional mismatch combined with the asymmetry and flexibility of the cations. Furthermore, the T_g values of the diether-substituted ILs increased gradually with the increase of chain length of the substituent, which might be attributed to an additional energy required to reorient larger cations in the glassy state.[34] In comparison with the T_g values of the reported ILs based on $[Co(C_2B_9H_{11})_2]^-$ (from –18 to –34 °C),[18] these new carborane-derivatized ILs with two alkoxy groups showed lower glass transition temperatures and were in a supercooled state for longer. Moreover, the heat capacity is a crucial parameter, which is very important in the fields of thermodynamics, thermochemistry, and industrial processes. From Table 1, it can be seen that the C_p values for the new ILs range from 1.99 J/g/K to 2.14 J/g/K at 25 °C, which are much higher than common ILs based on $[BF_4]^-$ and $[PF_6]^-$, e.g. at 25 °C the C_p of [BMIm][BF_4] and [BMIm][PF_6] are 1.56 J/g/K and 1.40 J/g/K, respectively.[35]

Figure 5 shows the TGA traces of five ILs based on the [*nido*-7,8-$C_2B_9H_{12}$]$^-$ anion and the starting *o*-carborane. In comparison with the *o*-carborane, which can completely sublime at 200 °C under a nitrogen atmosphere,[36] these carborane-derivatized ILs exhibited relatively good thermal stability. As shown from the curves in Figure 5, and the data in Table 1, the thermal decomposition temperatures (T_d) for the nine ILs ranged from 175 °C to 343 °C. Evidenced from the TGA profiles is the fact that with certain carborane anions, the thermal stability of the ILs depends strongly on the nature of the cation, i.e. the charge density, acidic proton, and expansionary force of the cation head group.[37] For instance, imidazolium and pyridinium salts are much more stable than these ether-functional ammonium salts, due to the graft of the ether group on the cation decreasing the thermal stabilities of the ILs.[38] The thermal stability of these ammonium salts generally increases in the order $[N_{111O1,2O2}]^+ < [N_{111O1,1O2}]^+ < [N_{111O2,2O2}]^+ < [N_{112O2,2O2}]^+ < [N_{111O2,1O2}]^+$, where $[N_{111O2,1O2}]$[*nido*-7,8-$C_2B_9H_{12}$] exhibited the highest T_d value of 232 °C. Moreover, an interesting phenomenon was observed from the TGA curves. That is, differing from most common ILs which are nearly decomposed completely under high temperature, the ILs based on [*nido*-7,8-$C_2B_9H_{12}$] showed ca. 30–80wt.-% weight loss, that is, 20–70% weight still can be retained even after being heated up to 800 °C. For example, [BPy][*nido*-7,8-$C_2B_9H_{12}$] began to decompose at 290 °C and only underwent 32wt.-% loss as the temperature rose to 800 °C, whereas the total weight loss of $[N_{112O2,2O2}]$[*nido*-7,8-$C_2B_9H_{12}$] was ca. 80wt.-% after the same heating process.

In order to investigate the component and the structure of the solid residues after calcination, three techniques were employed: SEM, XPS, and XRD. As shown in the SEM pictures (Figure 6, a and b), the residue resulting from the decomposition of $[N_{111O2,2O2}]$[*nido*-7,8-$C_2B_9H_{12}$] displayed an interesting morphology, with an approximately spherical, hollow, and reticular porous structure, which might derive from the expansion of the IL at high temperature, immediately followed by the release of large amounts volatile gas generated from the decomposition leaving the nonvolatile skeleton. This provides us with a new strategy for preparing new inorganic porous materials through the thermal decomposition of ILs. Furthermore, it is also helpful for understanding the pyrolysis mechanism of ILs. XPS analysis (Figure 6, c) showed that the residue of $[N_{111O2,2O2}]$[*nido*-7,8-$C_2B_9H_{12}$] was composed of four elements (B, C, O, and N). A trace of silicon as a contaminant was also detected. According to the high resolution spectrum of B 1s and O

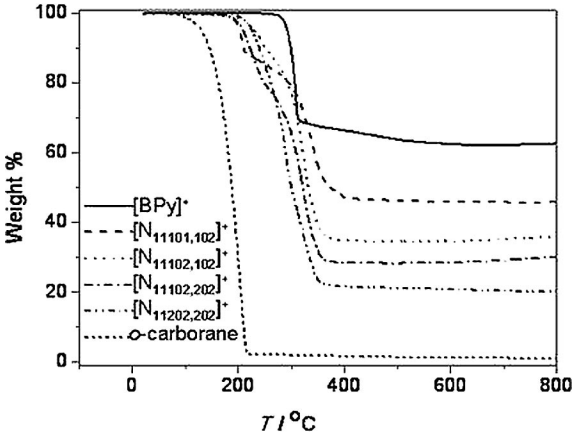

Figure 5. TGA traces of five carborane-based ILs.

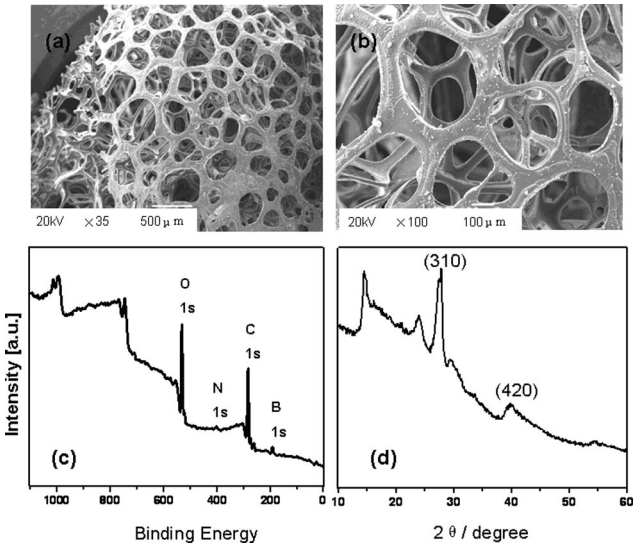

Figure 6. SEM images (a, b), XPS survey spectrum (c) and XRD pattern (d) of the $[N_{111O2,2O2}]$[*nido*-7,8-$C_2B_9H_{12}$] residue after calcination at high temperature.

1s, the most intense peaks centered at 194.0 and 533.6 eV, respectively, suggest that the B–O bonds are formed in the solid residue. In addition, another peak at B 1s was observed at 189.3 eV, which might reflect an area of B–B bonds in the residue.[39] From the C1s spectrum three peaks at 285.0, 287.2, and 290.0 eV were observed, which might originate from the C–C, C–N, and C–O bonds in the solid material, respectively.[40] From the XRD pattern (Figure 6, d) of the residue of $[N_{111O2,2O2}][nido\text{-}7,8\text{-}C_2B_9H_{12}]$, three strong peaks are observed at 2θ = 14.6, 27.7 (310), and 40.0° (420), respectively, which are characteristic of the cubic crystalline structure of boron oxide.[41] In combination with the XPS and XRD results, it can be seen that B_2O_3 and amorphous carbon are the main components of the skeleton.

Solubility

Table 2 lists the solubility of the carborane-derivatized ILs and *o*-carborane in some common solvents at room temperature. Firstly, almost all the carborane-derivatized ILs are easily soluble in many organic solvents including ethanol, acetone, methanol, acetonitrile, dichloromethane, chloroform, tetrahydrofuran, and dimethyl sulfoxide. Secondly, in comparison with the insolubility of [BMIm][*nido*-7,8-$C_2B_9H_{12}$], [BPy][*nido*-7,8-$C_2B_9H_{12}$], and [P14][*nido*-7,8-$C_2B_9H_{12}$] in water, the diether-functionalized ammonium salts with the [*nido*-7,8-$C_2B_9H_{12}$]$^-$ anion are partially miscible with water, which might be attributed to the improved hydrophilic characteristic of the ILs caused by introducing the ether group into the cations. Thirdly, similar to most ILs, all the carborane-derivatized ILs are completely immiscible with alkanes (e.g. hexane and cyclohexane); however, the *o*-carborane starting material is easily soluble in nonpolar solvents due to the lipophilic character of the cage.[42] Therefore, it can be concluded that, after the modification with the IL technique, the polarity of the carborane-derivatized organic salts was obviously enhanced, thereby resulting in the insolubility in alkanes.

Table 2. The solubility of prepared ILs and *o*-carborane in various solvents at room temp.

Solvent	Polarity index	Solubility [a] 1,2,3,4,5[b]	6,7,8,9[c]	*o*-carborane
Hexane	0.1	imisc	imisc	misc
Cyclohexane	0.2	imisc	imisc	misc
ethyl ether	2.8	imisc	imisc	misc
dichloromethane	3.1	misc	misc	misc
tetrahydrofuran	4.0	misc	misc	misc
Chloroform	4.1	misc	misc	misc
Methanol	5.1	misc	misc	misc
Acetone	5.1	misc	misc	misc
Ethanol	5.2	misc	misc	misc
Acetontrile	5.8	misc	misc	misc
Dimethyl sulfoxide	7.2	misc	misc	misc
Water	9.0	pm	imisc	imisc

[a] Misc = miscible; imisc = immiscible; pm = partially miscible. [b] Samples 1–5 are $[N_{112O2,2O2}][nido\text{-}7,8\text{-}C_2B_9H_{12}]$, $[N_{111O2,2O2}][nido\text{-}7,8\text{-}C_2B_9H_{12}]$, $[N_{111O1,2O2}][nido\text{-}7,8\text{-}C_2B_9H_{12}]$, $[N_{111O1,1O2}][nido\text{-}7,8\text{-}C_2B_9H_{12}]$, and $[N_{111O2,1O2}][nido\text{-}7,8\text{-}C_2B_9H_{12}]$, respectively. [c] Samples 6–8 are $[C_{1O2}MIm][nido\text{-}7,8\text{-}C_2B_9H_{12}]$,[P14][*nido*-7,8-$C_2B_9H_{12}$],[BPy][*nido*-7,8-$C_2B_9H_{12}$], and [BMIm][*nido*-7,8-$C_2B_9H_{12}$], respectively.

Density, Viscosity, and Refractive Index

The densities (ρ), viscosities (η), and refractive indices (n) of $[N_{112O2,2O2}][nido\text{-}7,8\text{-}C_2B_9H_{12}]$, $[N_{111O2,2O2}][nido\text{-}7,8\text{-}C_2B_9H_{12}]$, $[N_{111O1,2O2}][nido\text{-}7,8\text{-}C_2B_9H_{12}]$ and $[N_{111O1,1O2}][nido\text{-}7,8\text{-}C_2B_9H_{12}]$ were studied, and selected data at 25 °C are collected in Table 3.

Table 3. Densities (ρ), viscosities (η), conductivities (κ) and refractive indices (n) for four ILs based on [*nido*-7,8-$C_2B_9H_{12}$]$^-$ at 25 °C.

Entry	Cations	ρ [g/cm^3]	η [cP]	κ [μS/cm]	n
1	$[N_{112O2,2O2}]^+$	1.0094	1481	101	1.5244
2	$[N_{111O2,2O2}]^+$	1.0281	2194	87	1.5314
3	$[N_{111O1,2O2}]^+$	0.9900	798	233	1.5316
4	$[N_{111O1,1O2}]^+$	0.9938	1034	172	1.5449

In general, the density of the IL strongly depends on the symmetry of and the interaction forces between the cations and the anions. In comparison with common $[BF_4]^-$ ILs (e.g. [BMIm][BF_4] = 1.24 g/cm^3 at 25 °C)[35], the four carborane-derivatized RTILs displayed lower densities of 0.9900–1.0281 g/mL at 25 °C, which might be attributed to the special bulky carborane anion. The measured densities are also in agreement with previous results for $[CB_{11}H_{12}]^-$[15] and $[Co(C_2B_9H_{11})_2]^-$[18] imidazolium ILs. Moreover, the densities of the four RTILs based on [*nido*-7,8-$C_2B_9H_{12}$]$^-$ increased in the following cation order: $[N_{111O1,2O2}]^+ > [N_{111O1,1O2}]^+ > [N_{112O2,2O2}]^+ > [N_{111O2,2O2}]^+$, suggesting that the slight changes of the cation structure including the length of the alkyl chains, the cation size, and symmetry of the cation, results in some difference in their densities.

Although the four carborane-derivatized ILs are liquids at room temperature, their viscosities ranged from 798–2194 cP, which are higher than that of traditional ILs (e.g. the viscosity of [BMIm][BF_4] is 103 cP at 25 °C)[43] but much lower than that of liquid $[C_{12}MIm][Co(C_2B_9H_{11})_2]$ (9950 cP at 25 °C).[18] Despite the introduction of two ether groups into the cation decreasing the viscosities of the ILs due to the more flexible nature of the ether group, the highly delocalized charge, specific symmetry, and structural rigidity of the anionic boron clusters essentially determins the high viscosity of these carborane-derivatized ILs.[33] Of the four ILs, $[N_{111O1,1O2}][nido\text{-}7,8\text{-}C_2B_9H_{12}]$ displayed the lowest viscosity (798 cP at 25 °C), and the viscosities increased in the following order: $[N_{111O1,2O2}][nido\text{-}7,8\text{-}C_2B_9H_{12}] > [N_{111O1,1O2}][nido\text{-}7,8\text{-}C_2B_9H_{12}] > [N_{112O2,2O2}][nido\text{-}7,8\text{-}C_2B_9H_{12}] > [N_{111O2,2O2}][nido\text{-}7,8\text{-}C_2B_9H_{12}]$, indicating that the viscosity of these carborane-derivatized ILs is related to the length and freedom degree conformation of the substituent group of the corresponding cations.[44]

Moreover, compared to the refractive indices (n) of traditional ILs (e.g. n = 1.4188 for [BMIm][BF_4] and n = 1.4083 for [BMIm][PF_6] at 25 °C),[45] these carborane-derivatized ILs exhibit higher refractive indices, ranging from 1.5244

to 1.5449 at 25 °C. The refractive indices decreased with increasing the chain length of the cation, i.e. $[N_{112O2,2O2}]^+ < [N_{111O2,2O2}]^+ < [N_{111O1,2O2}]^+ < [N_{111O1,1O2}]^+$. According to the Lorenz–Lorentz equation (1).

$$(n^2 - 1)/(n^2 + 2) = 4\pi dNa/3M \quad (1)$$

where n is the refractive index value, d is the density, a is the polarizability, M is the molar mass and N is a constant, the high refractive indices of the carborane ILs originate from high polarizability of the [*nido*-7,8-$C_2B_9H_{12}$]$^-$ anion.

Electrochemical Properties

Since most of the reported ILs based on carborane anions are solids at room temperature, information related to their electrochemical properties is relatively scarce. Herein, the electrochemical properties of four carborane-derivatized RTILs including the ionic conductivity and the electrochemical stability were investigated. Of the four RTILs, [$N_{111O1,2O2}$][*nido*-7,8-$C_2B_9H_{12}$] gave the highest conductivity of only 233 μS/cm (Table 3), which is significantly lower than that of common ILs.[43] According to the conclusions drawn by Grätzel et al., ionic conductivity of an IL is mainly determined by its viscosity and ionic size.[46] The bulky [*nido*-7,8-$C_2B_9H_{12}$]$^-$ anion may decrease the rate of ion mobility and increase the viscosity, thereby resulting in the low conductivities of the ILs.

Furthermore, the electrochemical stability of the ILs was evaluated by cyclic voltammetry. From Figure 7, it can be seen that the three carborane-derivatized ILs exhibited the same oxidative potential at ca. 1.1 V, and their reductive potentials (from –0.8 to –2.4 V) were different due to the electrochemical stability of three cations. The cathodic limit values of the cations follow the order: [BPy] > [BMIm] > [$N_{112O2,2O2}$]. From the three cyclic voltammograms, an oxidative peak is observed at 1.5–1.6 V, indicating that one irreversible redox process occurs at this potential. Although the nature of the electrochemical oxidative process is not clear at this stage, it might be caused by the electrochemical reactivity of the [*nido*-7,8-$C_2B_9H_{12}$]$^-$ anion. In comparison with widely used IL electrolytes, these carborane-derivatized RTILs exhibit nonideal electrochemical stability, mainly due to the relatively high reactivity of the anion at the anode at voltages in excess of 1 V. This may limit their application as electrolytes in electrochemistry.

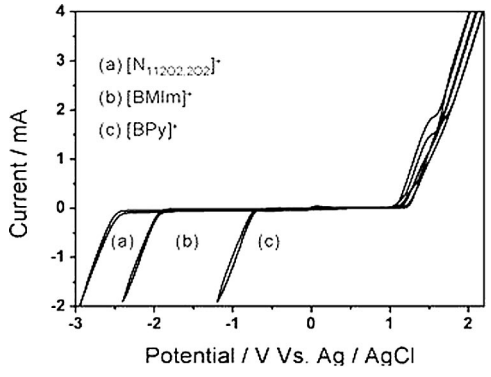

Figure 7. Cyclic voltammograms of three representative ILs based on [*nido*-7,8-$C_2B_9H_{12}$]$^-$.

Tribological Properties

It is known that ILs are good candidates for use as high-performance lubricants or additives in tribology because of their remarkable lubrication properties.[47] However, up to now, very few studies on the tribological performance of carborane-derivatized ILs have been reported. Thus, the tribological behavior of the carborane-based ILs as lubricants under variable conditions has also been studied.

Figure 8 gave a load ramp test stepped from 20 to 60 N with 10 N intervals at a frequency of 20 Hz for different ILs at room temperature, and the test duration for each load was 5 min. The results showed that the friction coefficients of the ILs decreased with increment of the load under the detected condition. For example, the friction coefficient of [$N_{112O2,2O2}$][*nido*-7,8-$C_2B_9H_{12}$] decreased from 0.185 to 0.155 with the load increasing from 20 to 60 N. A general order of friction coefficient values is observed as follows: $[N_{112O2,2O2}]^+ < [N_{111O2,2O2}]^+ < [N_{111O1,2O2}]^+ < [N_{111O1,1O2}]^+$, which is related to the length of the substituted chains of the corresponding cations. Moreover, the influence of constant loads on the tribological ability was also investigated. Figure 9 displays the evolution of the friction coefficient at a constant load of 60 N. The test duration in this experiment was 30 min at a frequency of 20 Hz. The friction coefficients of the carborane-derivatized ILs are in the range of 0.154–0.166 and keep relatively stable under constant loads. The order of friction coefficients under constant loads is in accordance with the results under variable loads, indicating that ILs with long substituted chains exhibit lower value of friction coefficient compared with those with short chains. Although these ILs based on carborane exhibited relatively high friction coefficient values than traditional ILs, such as $BMImBF_4$ (0.11),[48] good stability and duration of these materials as lubricants under rigorous friction conditions was observed.

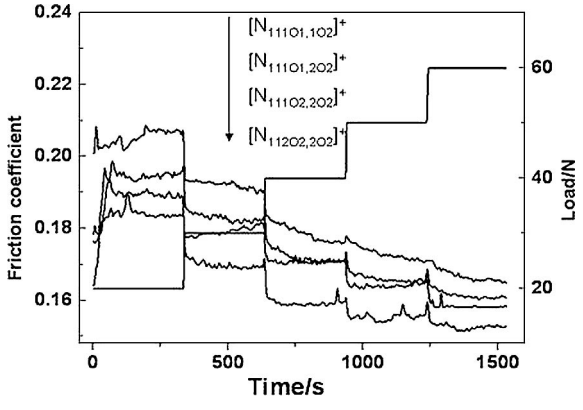

Figure 8. The evolution of friction coefficients with time during a load ramp test from 20 to 60 N (temperature: 25 °C, stroke: 1 mm, frequency: 20 Hz).

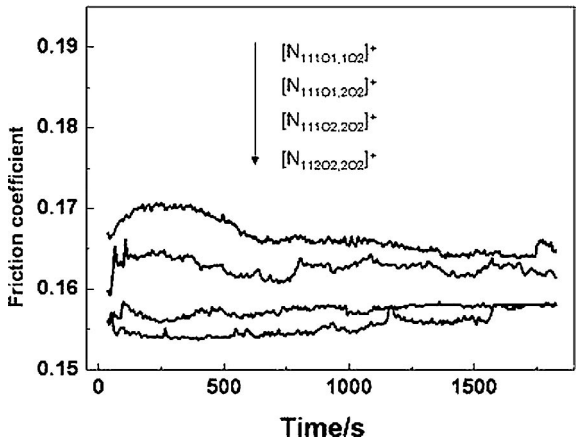

Figure 9. The evolution of friction coefficients with time at 60 N (temperature: 25 °C, stroke: 1 mm, frequency: 20 Hz, duration: 30 min).

Conclusions

A new class of diether-functionalized ammonium salts based on the [*nido*-7,8-$C_2B_9H_{12}$]$^-$ anion has been synthesized and characterized. Among these new ILs, four salts are viscous liquids at room temperature owing to the flexibility of alkoxy ether chains. TGA analysis showed that ca. 20–70wt.-% residues were maintained after calcination at high temperature. These residues were mainly composed of B_2O_3 and amorphous carbon and displayed interesting structures with hollow, reticular shell morphology. Moreover, the ILs based on [*nido*-7,8-$C_2B_9H_{12}$]$^-$ possess special physicochemical properties, such as relatively high heat capacity, high refractive index, low density, and good lubrication behavior. From a fundamental point of view, the emergence of these new RTILs based on carborane has a significance for boron chemistry and materials chemistry.

Experimental Section

Chemicals and Synthesis: *o*-carborane was purchased from Strem Chemicals Inc. (USA) and used as received. All other analytical grade reagents were used without further purification. The halide salts of [C_{1O2}MIm]$^+$, [P14]$^+$, [BPy]$^+$, [BMIm]$^+$ were prepared according to literature procedures.[49] The halide salts of diether-substituted ammonium were prepared by a similar method. Taking the synthesis of [$N_{112O2,2O2}$][*nido*-7,8-$C_2B_9H_{12}$] as an example, 2-bromoethyl ethyl ether was mixed with excess 33 wt.-% aqueous dimethylamine whilst stirring at 40 °C for 24 h. After neutralization with NaOH, NaCl was added to form a saturated solution. The mixture was distilled at 90 °C to obtain an azeotrope of 2-ethoxy-*N*,*N*-dimethylethanamine (N_{111O2}) and water. $CaCl_2$ was added to the azeotrope to remove the water, and the solution was filtered. The filtrate was washed three times with anhydrous ethyl ether and was distilled at 116 °C to obtain N_{112O2}. The quaternization reaction of N_{112O2} with 2-bromoethyl ethyl ether was conducted in ethanol at 80 °C for 48 h. After the removal of the volatile solvents and the unreacted reagents by rotary evaporation at 80 °C, a white solid was in 92% yield. Counterion exchange with an equimolar amount of Cs[nido-7,8-$C_2B_9H_{12}$] was performed in a mixture of chloroform and acetone (5:1 by volume). After filtration and the removal of volatile solvents, the resulting colorless viscous liquid was obtained and stored in a desiccator under dry nitrogen.

[$N_{112O2,2O2}$][*nido*-7,8-$C_2B_9H_{12}$]: [$N_{112O2,2O2}$]Br (5.1 g, 18.8 mmol) and Cs[*nido*-7,8-$C_2B_9H_{12}$] (5.0 g, 18.8 mmol) afforded a colorless liquid (5.6 g, 92%, yield 85% based on *o*-carborane). MW, 323.7. Br content: 0.18 wt.-%. Water content: 608 ppm. ^{1}H NMR (400 MHz, [D$_6$]acetone, 25 °C): δ = 4.00 (m, 4 H, 3-CH_2), 3.90 (m, 4 H, 2-CH_2), 3.59 (q, J = 6.9 Hz, 4 H, 4-CH_2), 3.43 (s, 6 H, 1-CH_3), 1.69 (s, $C_{cluster}$H), 1.19 (t, J = 7.0 Hz, 6 H, 5-CH_3), –2.95 (br. s, $C_{cluster}$H) ppm. ^{13}C NMR (100 MHz, [D$_6$]acetone, 25 °C): δ = 67.09, 65.38, 64.82, 53.02, 43.14–42.21 (br., $C_{cluster}$) 15.29 ppm. IR: $\tilde{\nu}$ = 3023, 2978, 2930, 2879, 2520, 1482, 1389, 1354, 1123, 1034, 963 cm^{-1}. MS (ESI$^+$): Calculated for [$C_{10}H_{24}NO_2$]$^+$: 190.1802; found 190.1806 (The serial numbers of carbon atoms for each ILs were given Figure S1–S9).

[$N_{111O2,2O2}$][*nido*-7,8-$C_2B_9H_{12}$]: [$N_{111O2,2O2}$]Br (4.9 g, 19.2 mmol) and Cs[*nido*-7,8-$C_2B_9H_{12}$] (5.1 g, 19.2 mmol) afforded a colorless liquid (5.6 g, 95%, yield 87% based on *o*-carborane). MW = 309.7. Br content: 0.15 wt.-%. Water content: 574 ppm. ^{1}H NMR (400 MHz, [D$_6$]acetone, 25 °C): δ = 4.01 (m, 4 H, 3,6-CH_2), 3.90 (m, 4 H, 2-CH_2), 3.59 (q, J = 6.9 Hz, 2 H, 4-CH_2), 3.43 (s, 6 H, 1-CH_3), 3.39 (s, 3 H, 7-CH_3), 1.69 (s, $C_{cluster}$H),1.18 (t, J = 7.0 Hz, 3 H, 5-CH_3), –2.96 (br. s, $C_{cluster}$H) ppm. ^{13}C NMR (100 MHz, [D$_6$]-acetone, 25 °C): δ = 67.10, 66.84, 65.35, 64.80, 58.94, 52.97, 43.14–42.14 (br., $C_{cluster}$), 15.29 ppm. IR: $\tilde{\nu}$ = 3019, 2981, 2933, 2891, 2523, 1475, 1376, 1123, 1030, 963 cm^{-1}. MS (ESI$^+$): Calculated for [$C_9H_{22}NO_2$]$^+$: 176.1645; found 176.1650.

[$N_{111O1,2O2}$][*nido*-7,8-$C_2B_9H_{12}$]: [$N_{111O1,2O2}$]Cl (3.7 g, 18.7 mmol) and Cs[*nido*-7,8-$C_2B_9H_{12}$] (5.0 g, 18.8 mmol) afforded a pale yellow liquid (5.2 g, 94%, yield 87% based on *o*-carborane). MW = 295.7. Water content: 751 ppm. ^{1}H NMR (400 MHz, [D$_6$]acetone, 25 °C): δ = 4.91 (s, 2 H, 6-CH_2), 3.98 (m, 2 H, 3-CH_3), 3.76 (s, 3 H, 7-CH_3), 3.61 (m, 4 H, 4,2-CH_2), 3.46 (s, 6 H, 1-CH_3), 1.71 (s, $C_{cluster}$H), 1.19 (t, J = 6.8 Hz, 3 H, 5-CH_3), –2.95 (br. s, $C_{cluster}$H) ppm. ^{13}C NMR (100 MHz, [D$_6$]acetone, 25 °C): δ = 93.68, 66.91, 63.56, 61.41, 48.77, 43.51–42.10 (br., $C_{cluster}$), 15.27 ppm. IR: $\tilde{\nu}$ = 3026, 2978, 2933, 2885, 2520, 1469, 1120, 1030 cm^{-1}. MS (ESI$^+$): Calculated for [$C_8H_{20}NO_2$]$^+$: 162.1489; found 162.1487.

[$N_{111O1,1O2}$][*nido*-7,8-$C_2B_9H_{12}$]: [$N_{111O1,1O2}$]Cl (3.4 g, 18.7 mmol) and Cs[*nido*-7,8-$C_2B_9H_{12}$] (5.0 g, 18.8 mmol) afforded a pale yellow liquid (4.7 g, 89%, yield 83% based on *o*-carborane). MW, 281.6. Water content: 478 ppm. ^{1}H NMR (400 MHz, [D$_6$]acetone, 25 °C): δ = 4.87 (s, 2 H, 5-CH_2), 3.95 (m, 2 H, 3-CH_2), 3.75, (s, 3 H, 6-CH_3), 3.73 (m, 2 H, 2-CH_2), 3.40 (s, 3 H, 4-CH_3), 3.32 (s, 6 H, 1-CH_3), 1.71 (s, $C_{cluster}$H), –2.94 (br. s, $C_{cluster}$H) ppm. ^{13}C NMR (100 MHz, [D$_6$]acetone, 25 °C): δ = 93.74, 66.27, 61.43, 58.98, 48.82, 43.14–42.14 (br., $C_{cluster}$) ppm. IR: $\tilde{\nu}$ = 3029, 2939, 2898, 2830, 2520, 1472, 1120, 1027 cm^{-1}. MS (ESI$^+$): Calculated for [$C_7H_{18}NO_2$]$^+$: 148.1332; found 148.1336.

[$N_{111O21O2}$][*nido*-7,8-$C_2B_9H_{12}$]: [$N_{111O2,1O2}$]Br (4.6 g, 19.1 mmol) and Cs[*nido*-7,8-$C_2B_9H_{12}$] (5.1 g, 19.2 mmol) afforded a white waxy solid (5.5 g, 96%, yield 90% based on *o*-carborane). MW = 295.7. Br content: 0.13 wt.-%. Water content: 574 ppm. ^{1}H NMR (400 MHz, [D$_6$]acetone, 25 °C): δ = 3.97 (m, 4 H, 3-CH_2), 3.89 (m, 4 H, 2-CH_2), 3.40 (s, 6 H, 4-CH_3), 3.38 (s, 6 H, 1-CH_3), 1.71 (s, $C_{cluster}$H), –2.95 (br. s, $C_{cluster}$H) ppm. ^{13}C NMR (100 MHz, [D$_6$]-acetone, 25 °C): δ = 66.79, 65.45, 58.95, 52.98, 42.44–42.11 (br., $C_{cluster}$) ppm. IR: $\tilde{\nu}$ = 3026, 2939, 2898, 2827, 2517, 1472, 1123, 1027 cm^{-1}. MS (ESI$^+$): Calculated for [$C_8H_{20}NO_2$]$^+$: 162.1489; found 162.1487.

[C_{1O2}MIm][*nido*-7,8-$C_2B_9H_{12}$]: [C_{1O2}MIm]Br (2.5 g, 11.3 mmol) and Cs[*nido*-7,8-$C_2B_9H_{12}$] (3.0 g, 11.3 mmol) afforded a white waxy solid (2.9 g, 94%, yield 87% based on *o*-carborane). MW = 274.6. Br content: 0.09 wt.-%. Water content: 738 ppm. ^{1}H NMR (400 MHz, [D_6]acetone, 25 °C): δ = 9.04 (s, 1 H, 1-CH), 7.75 (d, J = 1.6 Hz, 1 H, 2-CH), 7.72 (d, J = 1.6 Hz, 1 H, 3-CH), 4.56 (t, J = 5.0 Hz, 2 H, 6-CH_2), 4.10 (s, 3 H, 7-CH_3), 3.83 (t, J = 4.8 Hz, 2 H, 5-CH_2), 3.36 (s, 3 H, 4-CH_3), 1.70 (s, $C_{cluster}$H), –2.93 (br. s, $C_{cluster}$H) ppm. ^{13}C NMR (100 MHz, [D_6]acetone, 25 °C): δ = 137.77, 124.52, 123.96, 70.75, 58.92, 50.50, 42.76–42.10, 36.75 ppm. IR: $\tilde{\nu}$ = 3160, 3119, 3026, 2994, 2943, 2837, 2529, 1607, 1562, 1476, 1357, 1160, 1014, 838, 752 cm^{-1}. MS (ESI$^+$): Calculated for [$C_7H_{13}NO_2$]$^+$: 141.1022; found 141.1026.

[P14][*nido*-7,8-$C_2B_9H_{12}$]: [P_{14}]Br (2.5 g, 11.3 mmol) and Cs[*nido*-7,8-$C_2B_9H_{12}$] (3.0 g, 11.3 mmol) afforded a white waxy solid (2.9 g, 89%, yield 83% based on *o*-carborane). MW = 275.7. Br content: 0.16 wt.-%. Water content: 812 ppm. ^{1}H NMR (400 MHz, [D_6]acetone, 25 °C): δ = 3.71 (t, J = 13.2 Hz, 4 H, 2-CH_2), 3.60 (m, 2 H, 4-CH_2), 3.28 (s, 3 H, 1-CH_3) 2.32 (s, 4 H, 3-CH_2), 1.91 (m, 2 H, 4-CH_2), 1.70 (s, $C_{cluster}$H), 1.44 (m, 2 H, 5-CH_2), 0.98 (t, J = 7.6 Hz, 3 H, 7-CH_3), –2.93 (br. s, $C_{cluster}$H) ppm. ^{13}C NMR (100 MHz, [D_6]acetone, 25 °C): δ = 64.99, 64.70, 48.75, 11.52–40.79, 22.16, 20.20, 13.64 ppm. IR: $\tilde{\nu}$ = 3029, 2965, 2879, 2523, 1463, 1027, 925 cm^{-1}.

[BMIm][*nido*-7,8-$C_2B_9H_{12}$]: [BMIm]Br (1.6 g, 7.5 mmol) and Cs[*nido*-7,8-$C_2B_9H_{12}$] (2.0 g, 7.5 mmol) afforded a white waxy solid (2.0 g, 96%, yield 90% based on *o*-carborane). MW = 272.6. Br content: 0.13 wt.-%. Water content: 851 ppm. ^{1}H NMR (400 MHz, [D_6]acetone, 25 °C): δ = 9.41 (s, 1 H, 1-CH), 7.82 (d, J = 1.6 Hz, 1 H, 2-CH), 7.76 (d, J = 1.6 Hz, 1 H, 3-CH), 4.40 (t, J = 7.2 Hz, 2 H, 5-CH_2), 4.10 (s, 2 H, 4-CH_3), 1.96 (m, 2 H, 6-CH_2), 1.10 1.96 (m, 2 H, 7-CH_2) 1.70 (s, $C_{cluster}$H), 0.95 (t, J = 7.4 Hz, 3 H, 8-CH_3), –2.93 (br. s, $C_{cluster}$H) ppm. ^{13}C NMR (100 MHz, [D_6]acetone, 25 °C): δ = 137.77, 124.77, 123.40, 51.22, 43.2–42.2, 36.72, 32.81, 13.75 ppm. IR: $\tilde{\nu}$ = 3157, 3114, 2959, 2930, 2871, 2515, 1561, 1455, 1162, 1026, 817, 748 cm^{-1}.

[BPy][*nido*-7,8-$C_2B_9H_{12}$]: [BPy]Br (1.6 g, 7.4 mmol) and Cs[*nido*-7,8-$C_2B_9H_{12}$] (2.0 g, 7.5 mmol) afforded a white waxy solid (1.8 g, 91%, yield 85% based on *o*-carborane). MW = 269.6. Br content: 0.20 wt.-%. Water content: 967 ppm. ^{1}H NMR (400 MHz, [D_6]acetone, 25 °C): δ = 9.20 (d, J = 6.0 Hz, 2 H, 1-CH), 8.76 (t, J = 8.0 Hz, 1 H, 3-CH), 8.30 (t, J = 6.6 Hz, 2 H, 2-CH), 4.87 (t, J = 7.6 Hz, 2 H, 4-CH_2), 1.70 (s, $C_{cluster}$H), 2.06 (m, 2 H, 5-CH_2), 1.43 (m, 2 H, 6-CH_2), 0.97 (t, J = 7.4 Hz, 3 H, 7-CH_3), –2.83 (br. s, $C_{cluster}$H) ppm. ^{13}C NMR (100 MHz, [D_6]acetone, 25 °C): δ = 146.52, 145.45, 129.33, 62.50, 42.64–41.01, 33.77, 19.77, 13.45 ppm. IR: $\tilde{\nu}$ = 3084, 2958, 2930, 2871, 2505, 1632, 1497, 1484, 1166, 1027, 765, 681 cm^{-1}.

Characterization and Instruments: Before characterization the ILs were dried at 90–100 °C under a vacuum of 10^{-2}–10^{-3} mbar for 10 h to remove any organic impurities or water.

Water Content: The water content of the ILs was measured with a Metrohm 831 KF coulometer. Because the [*nido*-7,8-$C_2B_9H_{12}$]$^-$ anion reacts with iodine in methanol solution slowly, we selected the data of the point of inflexion on the titration curve. Fresh Karl Fischer reagent was used for each test process and the whole process was performed in N_2 atmosphere in a glove box.

Bromide Content: The bromide content was determined with a Mettler–Toledo Seven Multimeter with a bromide ion selective electrode.

NMR: ^{1}H and ^{13}C NMR spectra were measured with a Bruker AMX-400 NMR spectrometer in [D_6]acetone solutions, and ^{11}B {^{1}H} NMR spectra were recorded with a Bruker DRX-400 NMR spectrometer in acetone solutions. Chemical shift values for ^{1}H and ^{13}C NMR spectra were referenced to $SiMe_4$ and ^{11}B {^{1}H} NMR spectra were referenced to BF_3·OEt_2.

FTIR and Raman: FTIR spectra were performed with a Thermo Nicolet 5700 FTIR spectrophotometer in the region from 400–4000 cm^{-1}. The samples were analyzed as films between KBr plates. Raman analysis was conducted with a Nicolet 910 Raman spectrometer, and the ILs were examined in cylindrical sample tubes.

ESI-MS: Electrospray ionization mass spectra were recorded with a Bruker Daltonics APEX II 47e FTMS. The samples were dissolved in methanol. Anion mass spectrometry of [$N_{112O2,2O2}$][*nido*-7,8-$C_2B_9H_{12}$] is examined as the typical sample: Calculated for [$C_2B_9H_{12}$]$^-$ 134.1813; found 134.1810.

XPS, SEM, and XRD: X-ray Photoelectron Spectroscopy (XPS) analysis was performed with a VG ESCALAB 210 instrument with Mg-K_α source (1253.6 eV) and calibrated vs. the C 1s peak at 285.0 eV. A thin layer of the IL was deposited on a polycrystalline gold substrate. The micrographs of the residues were observed by EPMA-810 Scanning Electron Microscopy (SEM) after coating with gold. The X-ray diffraction (XRD) patterns of the solid residues were recorded with a Philips X′Pert Pro powder X-ray diffractometer. The diffraction angle of the diffractograms was in the range of 2θ = 10–80°.

Phase Transitions and Thermal Stability: The phase transitions and the measurements of the specific heat capacity were performed with a Mettler–Toledo DSC822e calorimeter and calibrated using indium and zinc. The DSC data were evaluated using the Mettler–Toledo STARe software version 7.01. The samples (10–20 mg) were sealed in a 40 μL aluminum pan with a pinhole at the top of the pan to expose the sample to a N_2 flow (50 mL min^{-1}) using an empty pan as the reference. DSC traces were typically scanned from 100 to –100 °C at speed of 10 °C min^{-1}, and then followed by the heating process at the same speed. The decomposition temperature (T_d) was recorded with 5% of mass loss by Pyris Diamond Perkin–Elmer TG/DTA at scan rate of 10 °C min^{-1} under a N_2 atmosphere (flow rate = 100 mL min^{-1}) and each IL was heated from room temperature to 800 °C.

Solubility: The solubility of the carborane ILs in various organic solvents was tested at room temperature and the solubility results were evaluated by adding the ILs or *o*-carborane into the solvents.

Measurement of the Viscosity, Density, and Refractive Index: The viscosity and density of each IL was examined with a Stabinger Viscosimeter SVM 3000/GR at 25 °C. The refractive indices of the samples were measured at 25 °C with a WAY-2s Abbé refractometer (Shanghai Precision & Scientific Instrument Co.), calibrated with deionized water.

Conductivity and Electrochemical Stability: The ion conductivity was measured by a Mettler–Toledo Seven Multimeter. Cyclic voltammetry was conducted using a CHI 660A Electrochemical Work Station. The working electrode was a glassy carbon electrode (3 mm diameter), the auxiliary electrode was a platinum wire and a Ag/AgCl electrode was used as a reference. The cyclic voltammogram of the ILs in 0.1 M acetonitrile solution was performed to ascertain the accessible electrochemical window at a scan rate of 0.05 V s^{-1} in the potential vs. Ag/AgCl electrode.

Tribological Properties: Tests of the tribological behavior of the ILs was carried out with an Optimol SRV-IV oscillating reciprocating friction and wear tester with a ball-on-disc configuration.

Supporting Information (see footnote on the first page of this article): Spectra of ^{1}H NMR, ^{13}C NMR, ^{11}B NMR, FTIR, FT-Raman, ESI-MS; traces of DSC, TGA and cyclic voltammograms for prepared ILs.

Acknowledgments

This work was supported by the National Natural Science Foundation of China (grant numbers 20533080, 21002107). We are grateful to Ms. Ling Gao, Li He, and Mr. Qixiu Zhu for their assistance in this work.

[1] a) R. D. Rogers, K. R. Seddon, *Science* **2003**, *302*, 792–793; b) T. Welton, *Chem. Rev.* **1999**, *99*, 2071–2083; c) P. Wasserscheid, T. Welton, *Ionic Liquids in Synthesis*, VCH, Weinheim, **2007**.
[2] a) P. Wasserscheid, W. Keim, *Angew. Chem. Int. Ed.* **2000**, *39*, 3772–3789; b) J. Huang, T. Jiang, B. Han, H. Gao, Y. Chang, G. Zhao, W. Wu, *Chem. Commun.* **2003**, *14*, 1654–1655; c) R. A. Sheldon, *Green Chem.* **2005**, *7*, 267–278; d) M. Ruta, G. Laurenczy, P. J. Dyson, L. Kiwi-Minsker, *J. Phys. Chem. C* **2008**, *112*, 17814–17819.
[3] a) P. Bonhôte, A.-P. Dias, M. Armand, N. Papageorgiou, K. Kalyanasundaram, M. Grätzel, *Inorg. Chem.* **1996**, *35*, 1168–1178; b) H. Shobukawa, H. Tokuda, Md. A. B. H. Susan, M. Watanabe, *Electrochim. Acta* **2005**, *50*, 3872–3877; c) M. Forsyth, J. Huang, D. R. MacFarlane, *J. Mater. Chem.* **2000**, *10*, 2259–2265; d) S. Graber, K. Doyle, M. Neuburger, C. E. Housecroft, E. C. Constable, R. D. Costa, E. Ortí, D. Repetto, H. J. Bolink, *J. Am. Chem. Soc.* **2008**, *130*, 14944–14945.
[4] B. Weyershausen, K. Lehmann, *Green Chem.* **2005**, *7*, 15–19.
[5] M. P. Scott, C. S. Brazel, M. G. Benton, J. W. Mays, J. D. Holbrey, R. D. Rogers, *Chem. Commun.* **2002**, *13*, 1370–1371.
[6] A. Chakraborty, D. Seth, D. Chakrabarty, P. Setua, N. Sarkar, *J. Phys. Chem. A* **2005**, *109*, 11110–11116.
[7] The Biotech/Life Sciences Portal, *A New Class of Materials: Ionic Liquids*,http://www.biopro.de/en/region/freiburg/magazin/01053/index.html (2007).
[8] a) L. He, L. Duan, J. Qiao, R. Wang, P. Wei, L. Wang, Y. Qiu, *Adv. Funct. Mater.* **2008**, *18*, 2123–2131; b) S. Tang, A. Babai, A.-V. Mudring, *Angew. Chem. Int. Ed.* **2008**, *47*, 7631–7634.
[9] a) B. Mallick, B. Balke, C. Felser, A.-V. Mudring, *Angew. Chem. Int. Ed.* **2008**, *47*, 7635–7638; b) S. Hayashi, H. Hamaguchi, *Chem. Lett.* **2004**, *33*, 1590–1591.
[10] a) B. A. Omotowa, B. S. Phillips, J. S. Zabinski, J. M. Shreeve, *Inorg. Chem.* **2004**, *43*, 5466–5471; b) M. Palacio, B. Bhushan, *Adv. Mater.* **2008**, *20*, 1194–1198.
[11] a) H. G. Joglekar, I. Rahman, B. D. Kulkarni, *Chem. Eng. Technol.* **2007**, *30*, 819–828; b) M. E. Van Valkenburg, R. L. Vaughn, M. Williams, J. S. Wilkes, *Thermochim. Acta* **2005**, *425*, 181–188.
[12] a) B. Štíbr, *Chem. Rev.* **1992**, *92*, 225–250; b) R. E. Williams, *Chem. Rev.* **1992**, *92*, 177–207.
[13] a) I. Krossing, I. Raabe, *Angew. Chem. Int. Ed.* **2004**, *43*, 2066–2090; b) D. J. Crowther, S. L. Borkowsky, D. Swenson, T. Y. Meyer, R. F. Jordan, *Organometallics* **1993**, *12*, 2897–2903.
[14] C. A. Reed, *Acc. Chem. Res.* **1998**, *31*, 133–139.
[15] A. S. Larsen, J. D. Holbrey, F. S. Tham, C. A. Reed, *J. Am. Chem. Soc.* **2000**, *122*, 7264–7272.
[16] Y. Zhu, C. Ching, K. Carpenter, R. Xu, S. Selvaratnam, N. S. Hosmane, J. A. Maguire, *Appl. Organomet. Chem.* **2003**, *17*, 346–350.
[17] J. Dymon, R. Wibby, J. Kleingardner, J. M. Tanski, I. A. Guzei, J. D. Holbrey, A. S. Larsen, *Dalton Trans.* **2008**, 2999–3006.
[18] M. Nieuwenhuyzen, K. R. Seddon, F. Teixidor, A. V. Puga, C. Viñas, *Inorg. Chem.* **2009**, *48*, 889–901.
[19] N. Matsumi, M. Miyamoto, K. Aoi, *J. Organomet. Chem.* **2009**, *694*, 1612–1616.
[20] a) H. Matsumoto, H. Sakaebe, K. Tatsumi, *J. Power Sources* **2005**, *146*, 45–50; b) H. Matsumoto, M. Yanagida, K. Tanimoto, M. Nomura, Y. Kitagawa, Y. Miyazaki, *Chem. Lett.* **2000**, *29*, 922–923.
[21] M. F. Hawthorne, T. D. Andrews, P. M. Garrett, F. P. Olsen, M. Reintjes, F. N. Tebbe, L. F. Warren Jr., P. A. Wegner, D. C. Young, *Inorg. Synth.* **1967**, *10*, 91–118.
[22] M. A. Fox, A. E. Goeta, J. A. K. Howard, A. K. Hughes, A. L. Johnson, D. A. Keen, K. Wade, C. C. Wilson, *Inorg. Chem.* **2001**, *40*, 173–175.
[23] J. Yoo, J.-W. Hwang, Y. Do, *Inorg. Chem.* **2001**, *40*, 568–570.
[24] a) H. Lee, T. Onak, J. Jaballas, U. Tran, T. U. Truong, H. T. To, *Inorg. Chim. Acta* **1999**, *289*, 11–19; b) A. Franken, J. D. Kennedy, *Inorg. Chem. Commun.* **2005**, *8*, 52–54.
[25] a) R. A. Wiesboeck, M. F. Hawthorne, *J. Am. Chem. Soc.* **1964**, *86*, 1642–1643; b) L. A. Leites, *Chem. Rev.* **1992**, *92*, 279–323.
[26] a) C. Kolbeck, M. Killian, F. Maier, N. Paape, P. Wasserscheid, H.-P. Steinrück, *Langmuir* **2008**, *24*, 9500–9507; b) V. Lockett, R. Sedev, C. Bassell, J. Ralston, *Phys. Chem. Chem. Phys.* **2008**, *10*, 1330–1335; c) E. F. Smith, I. J. Villar-Garcia, D. Briggs, P. Licence, *Chem. Commun.* **2005**, 5633–5635.
[27] a) E. F. Smith, F. J. M. Rutten, I. J. Villar-Garcia, D. Briggs, P. Licence, *Langmuir* **2006**, *22*, 9386–9392; b) J. M. Gottfried, F. Maier, J. Rossa, D. Gerhard, P. S. Schulz, P. Wasserscheid, H.-P. Steinrüeck, *Z. Phys. Chem.* **2006**, *220*, 1439–1453.
[28] E. A. Il′inchik, T. M. Polyanskaya, V. V. Volkov, *J. Struct. Chem.* **2007**, *48*, 300–309.
[29] a) A. González-Campo, B. Boury, F. Teixidor, R. Núñez, *Chem. Mater.* **2006**, *18*, 4344–4353; b) T. Baše, Z. Bastl, M. Šlouf, M. Klementová, J. Šubrt, A. Vetushka, M. Ledinský, A. Fejfar, J. Macháček, M. J. Carr, M. G. S. Londesborough, *J. Phys. Chem. C* **2008**, *112*, 14446–14455.
[30] a) D. R. MacFarlane, J. Huang, M. Forsyth, *Nature* **1999**, *402*, 792 –794; b) C. M. Forsyth, D. R. MacFarlane, J. J. Golding, J. Huang, J. Sun, M. Forsyth, *Chem. Mater.* **2002**, *14*, 2103 –2108.
[31] a) J. C. Dearden, *Sci. Total Environ.* **1991**, *109–110*, 59–68; b) R. J. C. Brown, R. F. C. Brown, *J. Chem. Educ.* **2000**, *77*, 724–731.
[32] Z.-B. Zhou, H. Matsumoto, K. Tatsumi, *Chem. Eur. J.* **2004**, *10*, 6581–6591.
[33] L. C. Branco, J. N. Rosa, J. J. M. Ramos, C. A. M. Afonso, *Chem. Eur. J.* **2002**, *8*, 3671–3677.
[34] A. E. Visser, J. D. Holbrey, R. D. Rogers, *Chem. Commun.* **2001**, 2484–2485.
[35] C. P. Fredlake, J. M. Crosthwaite, D. G. Hert, S. N. V. K. Aki, J. F. Brennecke, *J. Chem. Eng. Data* **2004**, *49*, 954–964.
[36] Y. Zhu, A. Parthiban, F. B. H. Kooli, *Catal. Today* **2004**, *96*, 143–146.
[37] S. Zhang, X. Lu, Y. Zhang, Q. Zhou, J. Sun, L. Han, G. Yue, X. Liu, W. Cheng, S. Li, *Ionic Liquids and Relative Process Design*, Springer, Berlin, Heidelberg, **2009**, p. 143–191.
[38] Z.-B. Zhou, H. Matsumoto, K. Tatsumi, *Chem. Eur. J.* **2006**, *12*, 2196–2212.
[39] H. Y. Wang, X. M. Wang, J. H. Wu, J. H. Li, Y. W. Yu, Y. Yang, and EAST vacuum group, Journal of Physics, Conference Series *100* (**2008**) 062011.
[40] a) R. Alexandrescu, F. Huisken, G. Pugna, A. Crunteanu, S. Petcu, S. Cojocaru, R. Cireasa, I. Morjan, *Appl. Phys. A* **1997**, *65*, 207–213; b) S. Kim, K.-J. Lee, Y. Seo, *Langmuir* **2002**, *18*, 6185–6192.
[41] a) J. A. Bigdeloo, A. M. Hadian, *Int. J. Recent Trends Eng.* **2009**, *1*, 176–180; b) D. M. Zhu, E. Kisi, *J. Aust. Ceram. Soc.* **2009**, *45*, 49–53.
[42] H. Nemoto, J. G. Wilson, H. Nakamura, Y. Yamamoto, *J. Org. Chem.* **1992**, *57*, 435–435.
[43] A. Noda, K. Hayamizu, M. Watanabe, *J. Phys. Chem. B* **2001**, *105*, 4603–4610.
[44] L. J. A. Siqueira, M. C. C. Ribeiro, *J. Phys. Chem. B* **2009**, *113*, 1074–1079.

[45] Q. Zhang, Z. Li, J. Zhang, S. Zhang, L. Zhu, J. Yang, X. Zhang, Y. Deng, *J. Phys. Chem. B* **2007**, *111*, 2864–2872.
[46] K. Hayamizu, S. Tsuzuki, S. Seki, Y. Ohno, H. Miyashiro, Y. Kobayashi, *J. Phys. Chem. B* **2008**, *112*, 1189–1197.
[47] a) C. F. Ye, W. M. Liu, Y. X. Chen, L. G. Yu, *Chem. Commun.* **2001**, *21*, 2244–2245; b) F. Zhou, Y. M. Liang, W. M. Liu, *Chem. Soc. Rev.* **2009**, *38*, 2590–2599.
[48] H. Kamimura, T. Kubo, I. Minami, S. Mori, *Tribology Int.* **2007**, *40*, 620–625.
[49] a) Q. Liu, M. H. A. Janssen, F. van Rantwijk, R. A. Sheldon, *Green Chem.* **2005**, *7*, 39–42; b) J. Golding, N. Hamid, D. R. MacFarlane, M. Forsyth, C. Forsyth, C. Collins, J. Huang, *Chem. Mater.* **2001**, *13*, 558–564; c) M. C. Law, K.-Y. Wong, T. H. Chan, *Green Chem.* **2002**, *4*, 328–330; d) P. J. Dyson, M. C. Grossel, N. Srinivasan, T. Vine, T. Welton, D. J. Williams, A. J. P. White, T. Zigras, *J. Chem. Soc., Dalton Trans.* **1997**, 3465–3469.

Received: December 24, 2010
Published Online: March 9, 2011

